



## Age-related and amyloid-beta-independent tau deposition and its downstream effects

Anika Wuestefeld,<sup>1</sup> Alexa Pichet Binette,<sup>1</sup> David Berron,<sup>1,2</sup> Nicola Spotorno,<sup>1</sup>  
 Danielle van Westen,<sup>3,4</sup> Erik Stomrud,<sup>1,5</sup> Niklas Mattsson-Carlsson,<sup>1,6,7</sup>  
 Olof Strandberg,<sup>1</sup> Ruben Smith,<sup>1,6</sup> Sebastian Palmqvist,<sup>1,5</sup> Trevor Glenn,<sup>8</sup>  
 Svenja Moes,<sup>9</sup> Michael Honer,<sup>9</sup> Konstantinos Arfanakis,<sup>10,11</sup> Lisa L. Barnes,<sup>10</sup>  
 David A. Bennett,<sup>10,12</sup> Julie A. Schneider,<sup>10,12</sup> Laura E. M. Wisse<sup>3,†</sup>  
 and Oskar Hansson<sup>1,5,†</sup>

†These authors contributed equally to this work.

See Therriault and Grothe (<https://doi.org/10.1093/brain/awad210>) for a scientific commentary on this article.

Amyloid- $\beta$  ( $A\beta$ ) is hypothesized to facilitate the spread of tau pathology beyond the medial temporal lobe. However, there is evidence that, independently of  $A\beta$ , age-related tau pathology might be present outside of the medial temporal lobe. We therefore aimed to study age-related  $A\beta$ -independent tau deposition outside the medial temporal lobe in two large cohorts and to investigate potential downstream effects of this on cognition and structural measures.

We included 545 cognitively unimpaired adults (40–92 years) from the BioFINDER-2 study (*in vivo*) and 639 (64–108 years) from the Rush Alzheimer's Disease Center cohorts (*ex vivo*). <sup>18</sup>F-RO948- and <sup>18</sup>F-flutemetamol-PET standardized uptake value ratios were calculated for regional tau and global/regional  $A\beta$  *in vivo*. Immunohistochemistry was used to estimate  $A\beta$  load and tangle density *ex vivo*. *In vivo* medial temporal lobe volumes (subiculum, cornu ammonis 1) and cortical thickness (entorhinal cortex, Brodmann area 35) were obtained using Automated Segmentation for Hippocampal Subfields packages. Thickness of early and late neocortical Alzheimer's disease regions was determined using FreeSurfer. Global cognition and episodic memory were estimated to quantify cognitive functioning.

*In vivo* age-related tau deposition was observed in the medial temporal lobe and in frontal and parietal cortical regions, which was statistically significant when adjusting for  $A\beta$ . This was also observed in individuals with low  $A\beta$  load. Tau deposition was negatively associated with cortical volumes and thickness in temporal and parietal regions independently of  $A\beta$ . The associations between age and cortical volume or thickness were partially mediated via tau in regions with early Alzheimer's disease pathology, i.e. early tau and/or  $A\beta$  pathology (subiculum/Brodmann area 35/precuneus/posterior cingulate). Finally, the associations between age and cognition were partially mediated via tau in Brodmann area 35, even when including  $A\beta$ -PET as covariate. Results were validated in the *ex vivo* cohort showing age-related and  $A\beta$ -independent increases in tau aggregates in and outside the medial temporal lobe. *Ex vivo* age-cognition associations were mediated by medial and inferior temporal tau tangle density, while correcting for  $A\beta$  density.

Taken together, our study provides support for primary age-related tauopathy even outside the medial temporal lobe *in vivo* and *ex vivo*, with downstream effects on structure and cognition. These results have implications for our understanding of the spreading of tau outside the medial temporal lobe, also in the context of Alzheimer's disease. Moreover, this study suggests the potential utility of tau-targeting treatments in primary age-related tauopathy, likely already in preclinical stages in individuals with low  $A\beta$  pathology.

Received November 14, 2022. Revised March 20, 2023. Accepted April 06, 2023. Advance access publication April 21, 2023

© The Author(s) 2023. Published by Oxford University Press on behalf of the Guarantors of Brain.

This is an Open Access article distributed under the terms of the Creative Commons Attribution-NonCommercial License (<https://creativecommons.org/licenses/by-nc/4.0/>), which permits non-commercial re-use, distribution, and reproduction in any medium, provided the original work is properly cited. For commercial re-use, please contact [journals.permissions@oup.com](mailto:journals.permissions@oup.com)

- 1 Clinical Memory Research Unit, Department of Clinical Sciences Malmö, Lund University, SE-222 42 Lund, Sweden
- 2 German Center for Neurodegenerative Diseases (DZNE), 39120 Magdeburg, Germany
- 3 Department of Diagnostic Radiology, Clinical Sciences, Lund University, SE-222 42 Lund, Sweden
- 4 Image and Function, Skåne University Hospital, SE-205 02 Malmö, Sweden
- 5 Memory Clinic, Skåne University Hospital, SE-205 02 Malmö, Sweden
- 6 Department of Neurology, Skåne University Hospital, SE-205 02 Malmö, Sweden
- 7 Wallenberg Center for Molecular Medicine, Lund University, 221 84 Lund, Sweden
- 8 Johns Hopkins University School of Medicine, Baltimore, MD 21287, USA
- 9 Roche Pharmaceutical Research and Early Development, Roche Innovation Center Basel, F. Hoffmann-La Roche Ltd, CH-4070 Basel, Switzerland
- 10 Rush Alzheimer's Disease Center, Rush University Medical Center, Chicago, IL 60612, USA
- 11 Department of Biomedical Engineering, Illinois Institute of Technology, Chicago, IL 60616, USA
- 12 Department of Neurological Sciences, Rush University Medical Center, Chicago, IL 60612, USA

Correspondence to: Laura Wisse, PhD,  
Department of Diagnostic Radiology,  
Lund University, Remissgatan 4, Room 14-520, SE-222 42 Lund, Sweden  
E-mail: lemwise@gmail.com

Correspondence may also be addressed to: Oskar Hansson, MD, PhD,  
Memory Clinic,  
Skåne University Hospital, SE-205 02 Malmö, Sweden  
E-mail: oskar.hansson@med.lu.se

Anika Wuestefeld, MSc  
Clinical Memory Research Unit, Department of Clinical Sciences Malmö,  
Lund University, Klinikgatan 28, Room C1103b, SE-222 42 Lund, Sweden  
E-mail: anika.wuestefeld@gmail.com

**Keywords:** tau-PET imaging; amyloid-beta; MRI; medial temporal lobe subregions; ageing; PART; autoradiography

## Introduction

Amyloid-beta (A $\beta$ ) plaques and tau neurofibrillary tangles, the primary hallmarks of Alzheimer's disease, can be present decades before the onset of symptoms.<sup>1,2</sup> According to the A $\beta$  cascade hypothesis, A $\beta$  accumulation is one of the earliest pathological changes to occur in Alzheimer's disease,<sup>3,4</sup> first appearing in the neocortex and spreading to the rest of the brain with disease progression.<sup>5</sup> Tau pathology (neurofibrillary tangles), on the other hand, occurs early in the medial temporal lobe (MTL) regions' transentorhinal and entorhinal cortex<sup>6</sup> before spreading to the neocortex with disease progression. This occurrence outside the MTL is hypothesized to be facilitated by A $\beta$ .<sup>7-9</sup>

In primary age-related tauopathy (PART), however, tau pathology is thought to be present and confined to the MTL in individuals without or with very low levels of A $\beta$  pathology.<sup>10</sup> PART has also been shown to be linked to neurodegeneration and memory decline,<sup>10-13</sup> but less severe than in Alzheimer's disease.<sup>10</sup> Interestingly, accumulating evidence from post-mortem and animal studies suggest that tau pathology in PART, thought to be independent of A $\beta$ , might be present even outside the MTL.<sup>14-17</sup> In addition, tau seeding activity, which is the transcellular propagation of tau protein seeds, may be widespread in the brain even with limited observed tau pathology.<sup>15,18-20</sup> Based on this evidence, it is possible that PART, even in the absence of A $\beta$  pathology, also occurs in regions outside the MTL. Prior *in vivo* PET studies have reported similar findings of age-related tau-PET uptake outside the MTL,<sup>21-23</sup> but not all.<sup>24</sup> However, most studies used first-generation tracers and, except for Lowe *et al.*,<sup>22</sup> had small sample

sizes. Thus, investigating this in a large cohort with a second-generation tracer with less off-target binding<sup>25</sup> is important. Additionally, less is known about downstream effects of age-related A $\beta$ -independent tau in this population, especially outside the MTL.

Based on this, we aimed first to assess age associations with A $\beta$ -independent tau deposition within and outside the MTL in a large sample of cognitively unimpaired older adults ( $n = 545$ ) and an A $\beta$ -negative subgroup ( $n = 418$ ). To this end, we investigated regions typically affected during either early, intermediate or late stages of Alzheimer's disease<sup>1</sup> and used a second-generation tau-PET tracer (<sup>18</sup>F-RO948). Second, to investigate potential downstream effects of age-related tau deposition in ageing, we assessed associations of tau-PET uptake with (i) measures of neurodegeneration within the same regions; (ii) global cognition and episodic memory; and (iii) whether these downstream effects of tau deposition are independent of global and regional A $\beta$  deposition. Third, to extend previous work, we aimed to replicate and validate the results *ex vivo* using an autopsy cohort with neuropathology data ( $n = 587$ ). Fourth, we aimed to examine the validity of the tau-PET tracer with *in vitro* autoradiography.

## Materials and methods

### Participants

#### BioFINDER cohort: *in vivo*

We included 545 cognitively unimpaired adults older than 40 years from the Swedish BioFINDER-2 study (NCT03174938), recruited 2017–22, who underwent MRI, A $\beta$ - and tau-PET. The study was approved

by the ethical review board in Lund, Sweden, and all study participants provided written informed consent. None of the included study participants fulfilled the diagnostic criteria for mild cognitive impairment or any type of dementia, determined after thorough clinical and cognitive assessment (described in Palmqvist et al.<sup>26</sup>). By design of the BioFINDER-2 study, cognitively unimpaired participants are enriched for APOE-ε4 allele carriership.<sup>26</sup>

### Harmonized RADC cohorts: *ex vivo*

We used the data of 639 cognitively unimpaired individuals from four Rush Alzheimer's Disease Center (RADC) cohort studies: Religious Orders Study; Rush Memory and Aging Project; Minority Aging Research Study; and African American Clinical Core.<sup>27</sup> None of the included participants fulfilled the diagnostic criteria for mild cognitive impairment or any type of dementia. Aβ status was based on semi-quantitative estimates of neuritic plaque density as recommended by the Consortium to Establish a Registry for Alzheimer's Disease (CERAD).<sup>28</sup> The study was approved by an Institutional Review Board of Rush University Medical Center, all participants signed an informed consent, and a repository consent to share data and biospecimens.<sup>29</sup>

### *In vitro* autoradiography in primary age-related tauopathy

To validate the tau-PET tracer for use in PART, we used tissue sections from fresh-frozen human brain with PART from Lund University, Sweden. This specimen was rated as Braak IV but showed no Aβ plaques deposition (CERAD neuritic plaque score<sup>30</sup> 0, Thal phase<sup>5</sup> 0). <sup>3</sup>H-RO948 was tritiated at Roche with a molar activity of 54.3 Ci/mmol and a radiochemical purity higher than 99%. The brain tissue sections were incubated with the radioligand (10 nM) in 50 mM Tris-HCl buffer pH 7.4 at room temperature for 30 min. After washing three times for 10 min at 4°C in 50 mM Tris-HCl buffer pH 7.4 and three quick dips in distilled H<sub>2</sub>O at 4°C, the sections were dried at 4°C for 3 h. The sections were placed in a FujiFilm Cassette (BAS 2025), exposed to a FujiFilm Imaging Plate (BAS-IP TR 2025) for 5 days and scanned with a FujiFilm IP reader (BAS-5000) with a resolution of 25 μm per pixel. The autoradiograms were visualized with the software MCID Analysis (v7.0, Imaging Research Inc.). Immunostaining for co-localization of tau aggregates with <sup>3</sup>H-RO948 binding was assessed on the same sections using tau-specific antibody AT8 (AT8-Fluor594) conjugated with Alexa594 (7.5 μg/ml). In addition, the Aβ-specific antibody MOAB-2 (MOAB2-Fluor488) conjugated with Alexa488 (5 μg/ml) was used to assess the absence of Aβ within the samples. DAPI (4',6-diamidino-2-phenylindole) staining was used to visualize nuclei of cells.

### BioFINDER imaging protocols

#### MRI

T<sub>1</sub>- and T<sub>2</sub>-weighted images were acquired on a Siemens MAGENTOM Prisma 3 T MRI scanner (Siemens Medical Solutions) with a 64-channel head coil. For T<sub>1</sub>-weighted images, a magnetization prepared-rapid gradient echo (MPRAGE) sequence [in-plane resolution = 1 × 1 mm<sup>2</sup>, slice thickness = 1 mm, repetition time (TR) = 1900ms, echo time (TE) = 2.54 ms, flip-angle = 9°] was used. The T<sub>2</sub>-weighted images were acquired with a turbo spin echo sequence (in-plane resolution = 0.4 × 0.4 mm<sup>2</sup>, slice thickness = 2 mm, TR = 8240 ms, TE = 52 ms, flip-angle = 150°).

### Tau- and Aβ-PET

Aβ- and tau-PET scans were acquired with a digital GE Discovery MI Scanner (General Electric Medical Systems). Tau-PET was performed 70–90 min post-injection of ~370 MBq of <sup>18</sup>F-RO948. Aβ-PET was performed 90–110 min post injection of ~185 MBq of <sup>18</sup>F-flutemetamol. The Swedish Medical Products Agency and the local Radiation Safety Committee at Skåne University Hospital, Sweden, approved the PET imaging.

### Structural MRI processing and analysis

Using the Automated Segmentation of Hippocampal Subfields (ASHS) packages for T<sub>1</sub>- and T<sub>2</sub>-weighted MR images,<sup>31</sup> MTL subregions were automatically segmented to obtain hippocampal subfield volumes (from T<sub>2</sub>-weighted MRI) and MTL cortical thickness (from T<sub>1</sub>-weighted MRI) measures<sup>32,33</sup> using a new atlas<sup>34</sup> (Supplementary material).

Four MTL regions were selected since they are assumed to be affected early by tau pathology: subiculum, cornu ammonis (CA) 1, entorhinal cortex (ERC) and Brodmann area (BA) 35 (≈transentorhinal cortex). Volumes for the hippocampal subregions (subiculum, CA1) were directly obtained from the ASHS segmentation, averaged across hemispheres and corrected for intracranial volume (using volume-to-intracranial volume fractions). ERC and BA35 thickness measures were obtained using the graph-based multi-template thickness analysis pipeline applied to the T<sub>1</sub>-ASHS segmentations<sup>32,35</sup> and averaged across hemispheres.

FreeSurfer 6.0 was used to parcellate the T<sub>1</sub>-weighted MRI images. We analysed cortical thickness, averaged across hemispheres, from eight regions of interest (ROIs) (<https://surfer.nmr.mgh.harvard.edu/>): superior-frontal, orbitofrontal, anterior cingulate, inferior temporal, supramarginal, lateral occipital and two composite regions composed of precuneus/posterior cingulate and a motor composite (pre- and post-central cortex; control region).

All ROIs correspond to early (ERC, BA35, CA1, subiculum, precuneus/posterior cingulate), intermediate (inferior temporal, orbitofrontal, anterior cingulate, supramarginal cortex) or late (superior frontal, lateral occipital) involvement of Alzheimer's disease pathologies during disease progression. Thus, this is based on either the early occurrence of tau (e.g. ERC) and/or Aβ pathology (e.g. precuneus/posterior cingulate).

### Tau-PET and Aβ-PET processing and analysis

Standardized uptake value ratio (SUVR) was calculated using an inferior cerebellar reference region for <sup>18</sup>F-RO948-PET (tau-PET)<sup>36</sup> and whole cerebellum for <sup>18</sup>F-flutemetamol-PET (Aβ-PET).<sup>37</sup> Using the geometric transfer matrix method,<sup>38</sup> partial volume correction was performed for both <sup>18</sup>F-RO948-PET and <sup>18</sup>F-flutemetamol-PET. See Leuzy et al.<sup>39</sup> for details of our processing pipeline.

For <sup>18</sup>F-flutemetamol, a neocortical composite SUVR was calculated comprising frontal, parietal and temporal lobe regions.<sup>40</sup> To determine Aβ status (low versus high), a cut-off of 1.03 SUVRs (corresponding to 11 centiloids) was used for global <sup>18</sup>F-flutemetamol-PET, previously determined by Gaussian mixture modelling.<sup>26</sup> For 11 individuals, no <sup>18</sup>F-flutemetamol-PET data were available, and in these cases Aβ status was determined based on CSF Aβ42/Aβ40 ratio (see 'CSF biomarkers' section). For <sup>18</sup>F-RO948-PET, a composite MTL SUVR was calculated using the neocortical MTL regions (ERC and BA35; here denoted ERC/BA35



tau-PET) and excluding the hippocampus to reduce the influence of off-target binding in the choroid plexus. We used putamen tau-PET SUVR in order to take potential off-target or non-specific binding into account.<sup>41</sup> For that purpose, we regressed out age effects on putamen tau-PET signal and used the resulting residuals as a covariate in all primary analyses when estimating regional tau-PET effects. Finally, tau-PET outliers were checked, and none were excluded.

### CSF biomarkers

Handling procedure and analysis of CSF followed standardized protocol.<sup>42,43</sup> The concentration of A $\beta$ 42 and A $\beta$ 40 was measured with the Roche Elecsys platform (Roche Diagnostics International Ltd.) as described by Hansson *et al.*<sup>44</sup> To determine A $\beta$  status, a cut-off of 0.080 (determined by Gaussian mixture modelling<sup>26</sup>) was used for CSF A $\beta$ 42/A $\beta$ 40 ratio in the 11 cases where <sup>18</sup>F-flutemetamol-PET was not available. Seventy-eight individuals did not have CSF A $\beta$ 42/A $\beta$ 40 ratio data and were excluded from analysis. CSF p-tau181<sup>45</sup> was measured using CSF electrochemiluminescence immunoassay on a fully automated cobase 601 instrument (Roche Diagnostics International Ltd.).

### Cognitive assessments

#### BioFINDER cohort: *in vivo*

For the BioFINDER cohort, a modified version of the Preclinical Alzheimer's Cognitive Composite 5 (mPACC5)<sup>46</sup> was calculated using the Mini-Mental State Examination,<sup>47</sup> Alzheimer's Disease Assessment Scale-Cognitive subscale (ADAS)<sup>48</sup> delayed word list recall (double-weighted), Symbol Digit Modalities test<sup>49</sup>, and animal fluency. For details, see Binette *et al.*<sup>50</sup> To examine episodic memory, we calculated the number of failures of the delayed recall and mean failures of the immediate recall of the ADAS word list (out of 10). All test scores were normalized based on the values of the A $\beta$ - subgroup and, if applicable, reversed (for episodic memory), so a higher score equaled better performance for the mPACC5 and episodic memory score.

#### Harmonized RADC cohorts: *ex vivo*

For the RADC cohort, global cognition closest to death was estimated using a z-score, based on the mean and standard deviation of the combined cohorts baseline visit, average of 19 tests from five cognitive domains (Supplementary material).<sup>51,52</sup> A value lower than zero indicates a score worse than the baseline average of the combined cohorts. Episodic memory closest to death was estimated in the same manner with seven tests (Supplementary material).

### Neuropathological assessment of RADC cohorts

All details concerning the neuropathological data have been described elsewhere.<sup>29,51,53</sup> A $\beta$  load and paired helical filament (PHF) tau tangle density information from immunohistochemistry were used for main analyses, following the National Institute on Aging guidelines for neuropathologic assessment.<sup>28</sup> The neuropathological data contains burden of A $\beta$  proteinopathy identified by immunohistochemistry using monoclonal antibodies against 1–40 and 1–42 A $\beta$ , 4G8 (1:9000; Covance Labs), 6F/3D (1:50; Dako North America Inc.) and 10D5 (1:600; Elan Pharmaceuticals). The overall score is based on percentage area of cortex in eight brain regions: hippocampus, ERC, midfrontal, inferior temporal, angular gyrus,

calcarine, anterior cingulate and superior frontal cortex.<sup>53</sup> Overall A $\beta$  pathology load was calculated as the mean square root transformation of the score in these eight regions. PHF tau tangle density was assessed by stereology. Overall tau pathology burden scores were calculated using immunohistochemistry with AT8, an antibody specific to phosphorylated tau, and the square root taken. CERAD estimates were generated from modified Bielschowsky-stained sections. As a semiquantitative measure of neurofibrillary tangles, Braak stages were determined with Bielschowsky silver staining in frontal, temporal, parietal, ERC and hippocampus.<sup>6,54</sup> A $\beta$  pathology was additionally quantified using Thal phases<sup>5</sup> for a subset of individuals. A high portion (31.4%) of individuals with low CERAD semiquantitative estimates of neuritic plaque density (no to possible Alzheimer's disease) was not quantified on Thal phases. Therefore, we used CERAD neuritic plaque scores to determine A $\beta$  status.

### Statistical analyses

Analyses were performed in R 4.0.2.<sup>55</sup> First, Pearson partial correlations were calculated ('ppcor' package<sup>56</sup>) to assess associations between (i) age and regional tau-PET including sex and age-independent putamen signal as covariates; and (ii) including sex, age-independent putamen signal, and regional A $\beta$ -PET as covariates. Note that the residual of the association of age and putamen SUVR was included to adjust for age-independent effects of potential off-target binding. Only tau- and A $\beta$ -PET measures within the same ROI were associated with each other. Analyses were repeated in the A $\beta$ - subgroup. Second, associations between ROI thickness/volume (i) with age (covariates: sex, A $\beta$ -PET); and (ii) with the corresponding regional tau-PET (covariates: sex, age-independent putamen signal, A $\beta$ -PET) were estimated individually. Again, analyses were repeated in the A $\beta$ - subgroup. Lastly, associations between regional tau-PET, age, regional thickness/volume, and cognitive measures were estimated (covariates: regional A $\beta$ -PET, sex, education). These analyses were repeated, including age as an additional covariate. To investigate the MTL tau only, an ERC/BA35 tau-PET composite was used. All P-values were reported after false discovery rate (FDR,  $P < 0.05$ , Benjamini-Hochberg procedure).

Second, mediation models were fitted ('lavaan' package,<sup>57</sup> bootstrapping = 500). First, we fitted mediation models with regional A $\beta$ -PET as the mediator of significant age-regional tau-PET SUVR associations (covariate: sex). Second, regional tau-PET SUVR as the mediator of significant age-volume/thickness associates was investigated (covariates: sex, regional A $\beta$ -PET). Third, regional tau-PET SUVR as the mediator of significant age-cognition associations was investigated (covariates: sex, education, regional A $\beta$ -PET).

The same analyses were performed in the neuropathological cohort, using partial Spearman rank correlations due to the nature of the data. The associations between (i) age and regional tau tangles (covariate: sex); (ii) age and regional tau tangles (covariates: sex, A $\beta$ ); (iii) age with global cognition or episodic memory (covariates: sex, education, A $\beta$ ); (iv) tangles with global cognition (covariate: sex, education); and (v) tangles with global cognition (covariates: sex, education, A $\beta$ ) in the whole sample and the A $\beta$ - subgroup were investigated. Additionally, we fitted mediation models investigating the mediating effects of regional tau tangles on the association of age and cognition.

Seven *in vivo* sensitivity analyses were performed. First, to potentially capture earlier A $\beta$  accumulation, we repeated the analyses using the CSF A $\beta$ 42/A $\beta$ 40 ratio as covariate. Second, we repeated

analyses using global A $\beta$ -PET as a covariate. Third, since the tau-PET tracer may show unspecific binding, we repeated the analyses excluding cases with high skull/meningeal binding (described in Pichet Binette et al.<sup>58</sup>). Fourth, we examine the associations between regional tau-PET and CSF p-tau181. Fifth, analyses were repeated including APOE- $\epsilon$ 4 carriership as a covariate. Sixth, while model assumptions for Pearson partial correlations were met, we used robust regression models<sup>59–61</sup> to examine robustness for significant associations. Two *ex vivo* sensitivity analyses were performed. First, we repeated analyses defining A $\beta$  status based on Thal phases. Second, we repeated analyses using global A $\beta$  burden.

## Data availability

Anonymized data from BioFINDER will be shared on request from a qualified academic investigator for the sole purpose of replicating procedures and results presented in the article and as long as the data transfer is in agreement with EU legislation on the general data protection regulation and decisions by the Swedish Ethical Review Authority and Region Skåne, which should be regulated in a material transfer agreement.

A request to receive the data of the RADC cohorts can be submitted under: <https://www.radc.rush.edu/>.

## Results

### Demographics

Demographics of the *in vivo* cohort with cognitively unimpaired older adults ( $n = 545$ , 53% female, mean age 65, mean education 13 years, 49% APOE- $\epsilon$ 4 carriers), the *in vivo* A $\beta$ - subgroup ( $n = 418$ , 52% female, mean age 61, mean education 13 years, 42% APOE- $\epsilon$ 4 carriers; Table 1) and of the neuropathological dataset ( $n = 639$ , mean age  $87.4 \pm 7.00$ , 33% female, mean education 16 years) can be found in Table 1 and Supplementary Tables 1 and 2.

### Autoradiography

The <sup>3</sup>H-RO948-PET tracer was validated *in vitro* with autoradiography using cortical tissue sections from a PART case (Fig. 1). The results show that the tracer binds to tau pathology (based on AT8 staining) in the parahippocampal gyrus even in the absence of A $\beta$  pathology.

### A $\beta$ -independent associations of age and regional tau-PET signal within and outside the MTL

#### *In vivo*: BioFINDER-2 cohort

We first investigated the association between age and regional tau-PET signal in the whole sample. Age was positively associated with regional tau-PET signal in the MTL ( $r_p = 0.36$ ,  $P_{FDR} < 0.001$ ), as well as widespread neocortical ROIs (inferior temporal, superior frontal, orbitofrontal, anterior cingulate, posterior cingulate/precuneus, supramarginal and lateral occipital;  $r_p = 0.15–0.36$ ,  $P_{FDR} < 0.001$ ), adjusting for sex and tau-PET off-target putamen binding (Fig. 2A).

To examine if these associations are independent of A $\beta$ , we adjusted the age and regional tau-PET associations for regional A $\beta$ -PET signal (Fig. 2B and Supplementary Table 3). Age was still positively associated with medial temporal tau-PET ( $r_p = 0.24$ ,  $P_{FDR} < 0.001$ ) and interestingly, although with relatively small effect sizes, also with superior frontal, orbitofrontal, anterior cingulate,

**Table 1** Sample characteristics of the BioFINDER (*in vivo*) and the RADC (*ex vivo*) cohorts for the whole cognitively unimpaired and A $\beta$ - subgroup

BioFINDER cohort	Whole sample	A $\beta$ - <sup>a</sup>
<i>n</i>	545	418
Sex, % female	52.6	52.3
Age, years	65.0 $\pm$ 11.7 [40–92]	60.9 $\pm$ 11.5 [40–88]
APOE- $\epsilon$ 4 carrier, %	48.6	42.3
Education, years	12.8 $\pm$ 3.4	12.9 $\pm$ 3.3
mPACC5, z-scored	0.06 $\pm$ 0.81	0.17 $\pm$ 0.76
Episodic memory, z-scored	–0.23 $\pm$ 1.89	0.01 $\pm$ 1.81
CSF A $\beta$ 42/A $\beta$ 40 ratio	0.10 $\pm$ 0.028	0.11 $\pm$ 0.02
Global A $\beta$ -PET SUVR	1.01 $\pm$ 0.35	0.85 $\pm$ 0.06
ERC/BA35 tau-PET SUVR	1.19 $\pm$ 0.49	1.05 $\pm$ 0.32
RADC cohorts	Whole sample	A $\beta$ - <sup>b</sup>
<i>n</i>	639	318
Sex, <i>n</i> (% female)	205 (32.1)	112 (35.2)
Age at death, years	87.2 $\pm$ 7.2 [64–108]	86.0 $\pm$ 7.5 [64–108]
Education, years	16.3 $\pm$ 3.7	16.1 $\pm$ 3.7
APOE- $\epsilon$ 4 carrier, <i>n</i> (%)	93 (16)	35 (11.0)
Braak stages, <i>n</i> (%)		
0	15 (2.4)	11 (3.5)
I	63 (9.9)	51 (16.0)
II	105 (16.5)	75 (23.6)
III	210 (32.9)	116 (36.5)
IV	198 (31.0)	–
V	47 (7.4)	–
VI	–	–
CERAD, <i>n</i> (%)		
Definite	103 (16.1)	–
Probable	218 (34.0)	–
Possible	71 (11.1)	71 (22.3)
No Alzheimer's disease	247 (38.7)	247 (77.7)
Thal phase, <i>n</i> (%)		
0	84 (12.9)	84 (26.1)
1	110 (16.9)	92 (28.6)
2	27 (4.2)	16 (5.0)
3	188 (29.0)	22 (6.8)
4	82 (12.6)	3 (0.9)
5	53 (8.2)	4 (1.2)
A $\beta$ load, mean	1.12 $\pm$ 1.04	0.36 $\pm$ 0.57
Total tangle density, mean	3.33 $\pm$ 3.78	2.24 $\pm$ 2.38
Global cognition, z-scored	0.14 $\pm$ 0.45	0.20 $\pm$ 0.44
Episodic memory, z-scored	0.38 $\pm$ 0.57	0.44 $\pm$ 0.53

Continuous variables are displayed as mean  $\pm$  standard deviation; age range is presented within square brackets. Categorical variables are displayed as *n* (%). mPACC5 = modified Preclinical Alzheimer's Cognitive Composite; RADC = Rush Alzheimer's Disease Center; SUVR = standardized uptake value ratio.

<sup>a</sup>A $\beta$ - is defined, in BioFINDER, as a global SUVR  $< 1.03$  or  $< 0.08$  on CSF A $\beta$ 42/A $\beta$ 40 ratio if PET was not available.

<sup>b</sup>In the RADC cohorts, the A $\beta$ - subgroup is based on semiquantitative estimates of neuritic plaque density as recommended by the Consortium to Establish a Registry for Alzheimer's Disease (CERAD). Sensitivity analyses are done defining the A $\beta$ - subgroup according to Thal phases (0–1).

precuneus/posterior cingulate, and motor cortex tau-PET ( $r_p = 0.11–0.27$ ,  $P_{FDR} = 0.023–< 0.001$ ), regions typically not implicated in early tau deposition. Mediation models show similar results (Supplementary Fig. 1).

In the A $\beta$ - subgroup similar widespread associations between age and regional tau-PET tracer uptake were observed (Fig. 2E and F;  $r_p = 0.14–0.46$ ,  $P_{FDR} = 0.007–< 0.001$ ), with the largest effect sizes for precuneus/posterior cingulate and ERC/BA35 and smallest effect sizes for inferior temporal, supramarginal and lateral occipital

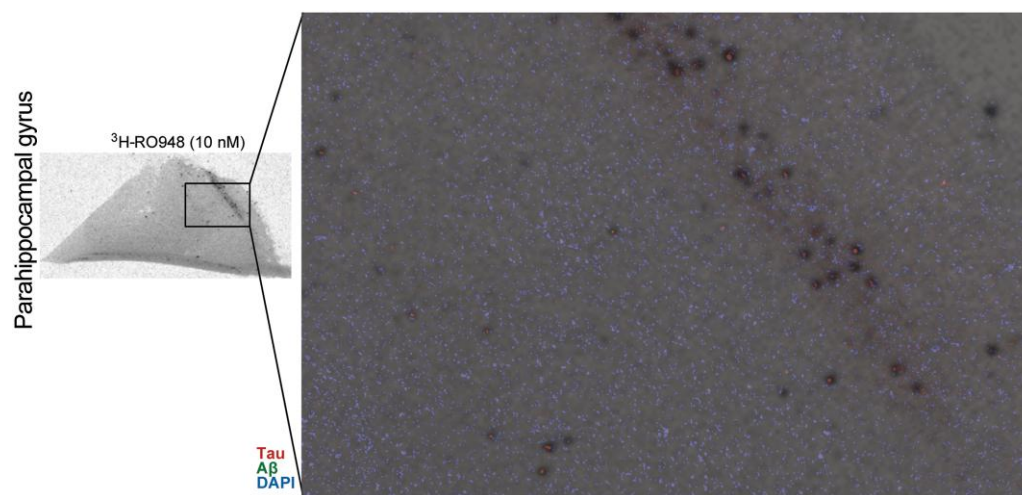


Figure 1  $^3\text{H-RO948}$  binds to tau pathology in the parahippocampal gyrus in PART. DAPI = 4',6-diamidino-2-phenylindole.

cortex. All associations remained statistically significant when adjusting for regional A $\beta$ -PET ( $r_p = 0.12\text{--}0.42$ ,  $P_{\text{FDR}} = 0.022\text{--}<0.001$ ), except for motor cortex tau-PET.

#### Ex vivo: RADC cohort

In the neuropathological dataset, age and tau tangle score were positively associated for all regions except lateral occipital tau tangles (Supplementary Table 6;  $\rho_{\text{OP}} = 0.10\text{--}0.39$ ,  $P_{\text{FDR}} = 0.020\text{--}<0.001$ ). After adjusting for regional A $\beta$  load, age was significantly associated with CA1 and ERC tau tangles and with smaller effect sizes to inferior temporal and anterior cingulate cortex tau tangle load (Fig. 2C and D;  $\rho_{\text{OP}} = 0.11\text{--}0.37$ ,  $P_{\text{FDR}} = 0.024\text{--}<0.001$ ). This supports the *in vivo* results of potential A $\beta$ -independent age-related tau deposition within and outside the MTL.

In the A $\beta$ - subgroup, A $\beta$ -independent associations between age and tau tangles were found for CA1 and entorhinal, inferior temporal, and anterior cingulate cortex, suggesting a potential age-tau tangle association in and outside the MTL ( $\rho_{\text{OP}} = 0.15\text{--}0.39$ ,  $P_{\text{FDR}} = 0.032\text{--}<0.001$ ), where weaker, but statistically significant correlations were observed for the latter two. It should be noted that tau tangle burden was not available for parietal regions (Fig. 2).

#### Association between age and regional structural measures is partially mediated by tau-PET signal

In the next step we investigated the associations of tau-PET SUVR with regional volume and ROI thickness, while adjusting for sex, regional A $\beta$ -PET, and the off-target variable (Fig. 3A and for details see Supplementary Table 7). Higher ERC/BA35 tau-PET SUVR was associated with lower subiculum ( $r_p = -0.30$ ,  $P_{\text{FDR}} < 0.001$ ) and CA1 ( $r_p = -0.19$ ,  $P_{\text{FDR}} = 0.002$ ) volume and BA35 thickness ( $r_p = -0.24$ ,  $P_{\text{FDR}} < 0.001$ ; Fig. 3A). For neocortical regions, higher regional tau-PET SUVR was associated with lower cortical thickness for inferior temporal cortex ( $r_p = -0.15$ ,  $P_{\text{FDR}} = 0.002$ ) and, regions typically associated with early A $\beta$  accumulation, precuneus/posterior cingulate cortex ( $r_p = -0.20$ ,  $P_{\text{FDR}} < 0.001$ ; Fig. 3A). This suggests potential A $\beta$ -PET-independent associations between tau-PET signal and neurodegeneration in these regions. While not focus of this paper, we adjusted the analyses for age and found that the results remained significant. This indicates that there are also age-independent tau-PET and volume/thickness relationships (Fig. 3B).

To further focus on the role of age in the tau and volume/thickness relationships, we examined whether tau-PET signal mediates the association between age and structure volume/thickness (Fig. 3D). The mediation models indicate that regional tau-PET partially mediates this association in an A $\beta$ -independent manner for subiculum ( $c\text{'-}c' = -0.06$ , 95% CI:  $-0.08\text{--}0.03$ ,  $P < 0.001$ , 15%) and BA35 ( $c\text{'-}c' = -0.04$ , 95% CI:  $-0.06\text{--}0.02$ ,  $P = 0.001$ , 15%), and for precuneus and posterior cingulate in the whole cognitively unimpaired sample ( $c\text{'-}c' = -0.02$ , 95% CI:  $-0.03\text{--}0.01$ ,  $P = 0.034$ , 5%; Fig. 3D). Note that the tau-PET mediating effects explained only a small portion of the variance of the age-structure relationship.

In the A $\beta$ - subgroup, higher ERC/BA35 tau-PET was significantly associated with lower volume in subiculum ( $r_p = -0.23$ ,  $P_{\text{FDR}} < 0.001$ ) and CA1 ( $r_p = -0.18$ ,  $P_{\text{FDR}} = 0.003$ ), and lower BA35 ( $r_p = -0.30$ ,  $P_{\text{FDR}} < 0.001$ ) and ERC ( $r_p = -0.12$ ,  $P_{\text{FDR}} < 0.001$ ) thickness; higher precuneus/posterior cingulate tau-PET was associated with reduced thickness in that region ( $r_p = -0.19$ ,  $P_{\text{FDR}} < 0.001$ ; Fig. 3 and Supplementary Table 7), again adjusting for A $\beta$ -PET and sex. This indicates direct regional tau-PET effects of the age-structure association appear to be A $\beta$ -independent for these regions. The association between ERC/BA35 tau-PET and BA35 and ERC thickness survived adjusting for age. Mediation models examining the role of age in the tau and volume/thickness relationships in this subgroup, indicate that ERC/BA35 tau-PET partially mediates the association between age and regional volume/thickness for BA35 ( $c\text{'-}c' = -0.06$ , 95%CI:  $-0.09\text{--}0.03$ ,  $P < 0.001$ , 18%; Fig. 3F).

#### MTL tau-PET signal partially mediates the association between age and global cognition

##### In vivo: BioFINDER-2 cohort

Next, we explored the association of imaging measures and cognitive performance (global cognition and episodic memory). Analyses were only conducted for regions with significant A $\beta$ -independent effects of tau-PET signal on volume/thickness (i.e. subiculum, CA1, BA35, inferior temporal, and precuneus/posterior cingulate cortex; Fig. 4).

In the whole sample of cognitively unimpaired older adults, significant associations with global cognition (mPACC5) and episodic memory were found for higher age, ERC/BA35 tau-PET, subiculum and CA1 volume, and BA35, inferior temporal, and precuneus/



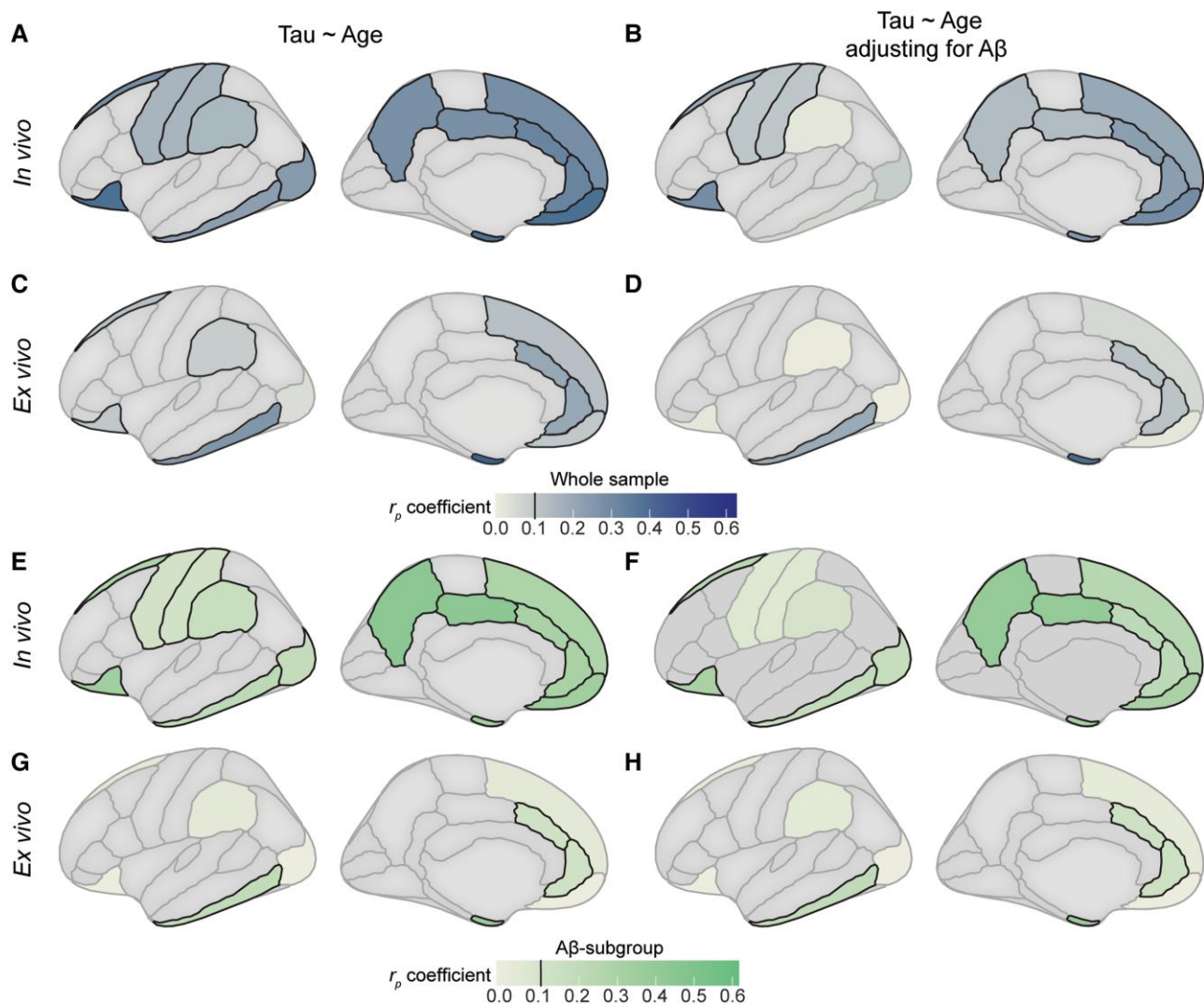


**Figure 2** Association between age and regional tau-PET  $^{18}\text{F}$ -RO948 uptake (*in vivo*) or regional tau tangles (*ex vivo*) in the whole samples and A $\beta$ - subgroups. (A) Increasing age is associated with increased regional tau-PET  $^{18}\text{F}$ -RO948 tracer uptake in medial temporal, parietal, and frontal regions. (B) A $\beta$ -PET independent associations between age and regional tau-PET signal in regions from A. (C) Increasing age is associated with increased regional tau tangles in medial temporal, parietal and frontal regions. (D) A $\beta$ -PET independent associations between age and regional tau tangles in temporal and frontal regions. E–H show the results of the same analysis as A–D but in the A $\beta$ - subgroup. Pearson partial correlation coefficients/Spearman rank correlations  $> 0.10$  are  $P_{\text{FDR}} < 0.05$  (dark outline). Light grey regions were not investigated. Similar results are found using global A $\beta$ -PET.

posterior cingulate thickness (see [Supplementary Table 8](#) for details). Higher inferior temporal and precuneus/posterior cingulate tau-PET SUVRs were only associated with reduced global cognition but not episodic memory. Most of these correlations were relatively weak. While, again, not primary focus of this paper, when additionally adjusting for age, only ERC/BA35 tau-PET was significantly associated with reduced global cognition and episodic memory scores ( $r_p = -0.16$ ,  $P_{\text{FDR}} = 0.001$ ;  $r_p = -0.14$ ,  $P_{\text{FDR}} = 0.002$ ). This suggests that there is also an age-independent association between ERC/BA35 tau-PET and cognition.

Further focusing on the role of age in the tau and cognition relationship, we performed mediation analyses of the age-cognition association with ERC/BA35 tau-PET. Similar to the mediation models of age-thickness/volume associations, mediation models showed that there is a partial mediation of ERC/BA35 tau-PET on the age-global cognition association ([Fig. 4B](#);  $c-c' = -0.04$ , 95% CI:  $-0.06$ :  $-0.01$ ,  $P = 0.002$ , 10%) partially independent of A $\beta$ . Mediations of

the association between age and episodic memory showed a partial mediation of ERC/BA35 tau-PET, independent of regional A $\beta$ , sex, and education ([Fig. 4D](#);  $c-c' = -0.03$ , 95% CI:  $-0.06$ :  $-0.01$ ,  $P = 0.013$ , 9%). These partial mediations hold also when adding subiculum volume or BA35 thickness as a covariate, indicating that this is independent of atrophy in these regions. Imaging measures in other regions were not associated with the cognition measures ([Supplementary Table 8](#)). Again, it should be noted that only a small portion of the variance of the age-cognition relationship was explained by the mediating effects of tau-PET.

In the A $\beta$ - subgroup, higher age was significantly associated with global cognition ( $r_p = -0.36$ ,  $P_{\text{FDR}} < 0.001$ ) and episodic memory ( $r_p = -0.26$ ,  $P_{\text{FDR}} < 0.001$ ). Higher ERC/BA35 and precuneus/posterior cingulate tau-PET were significantly associated with reduced global cognition ([Supplementary Table 8](#)). ERC/BA35 tau-PET was also significantly associated with reduced episodic memory. Subiculum and CA1 volume, as well as BA35, inferior

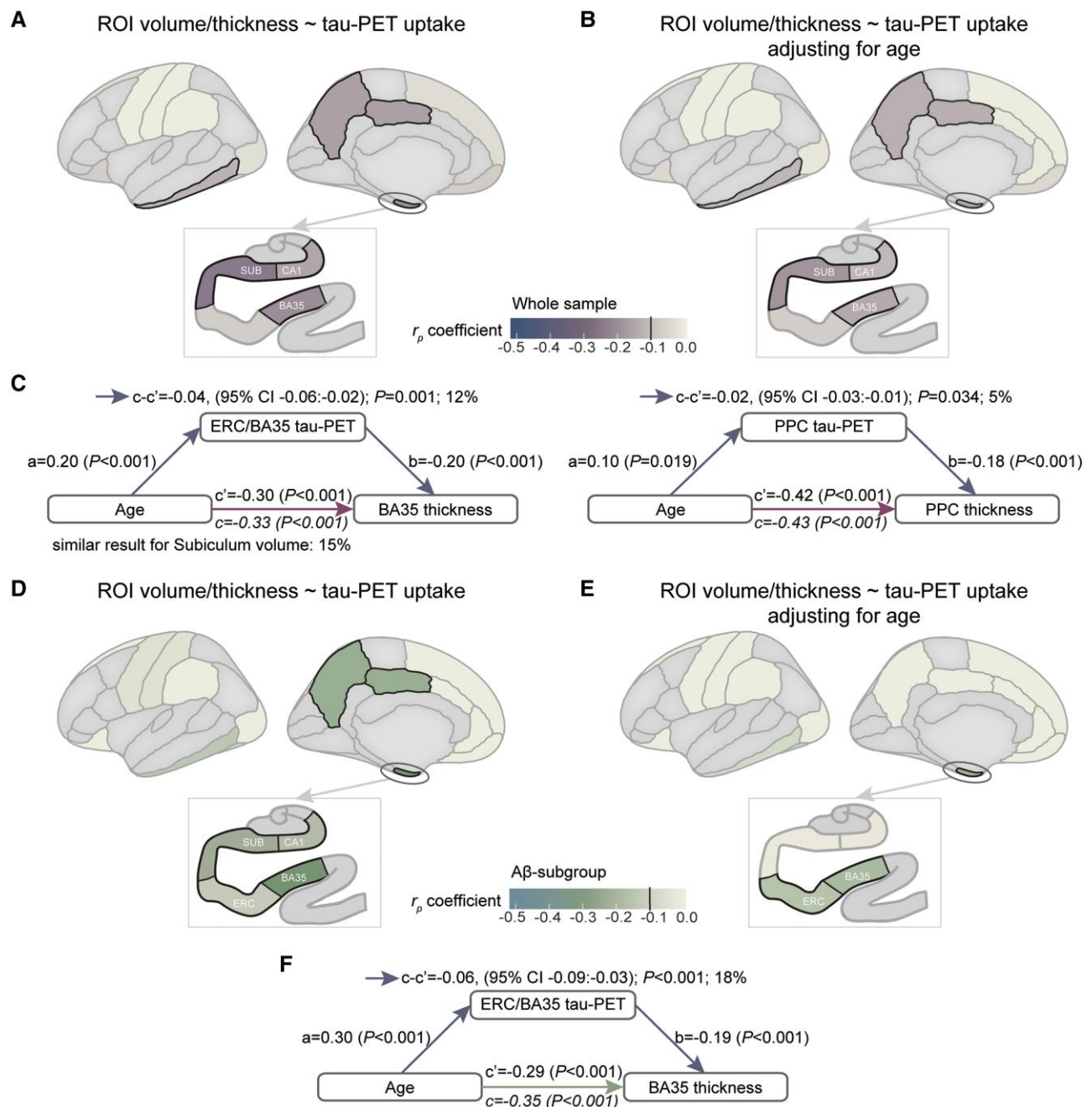


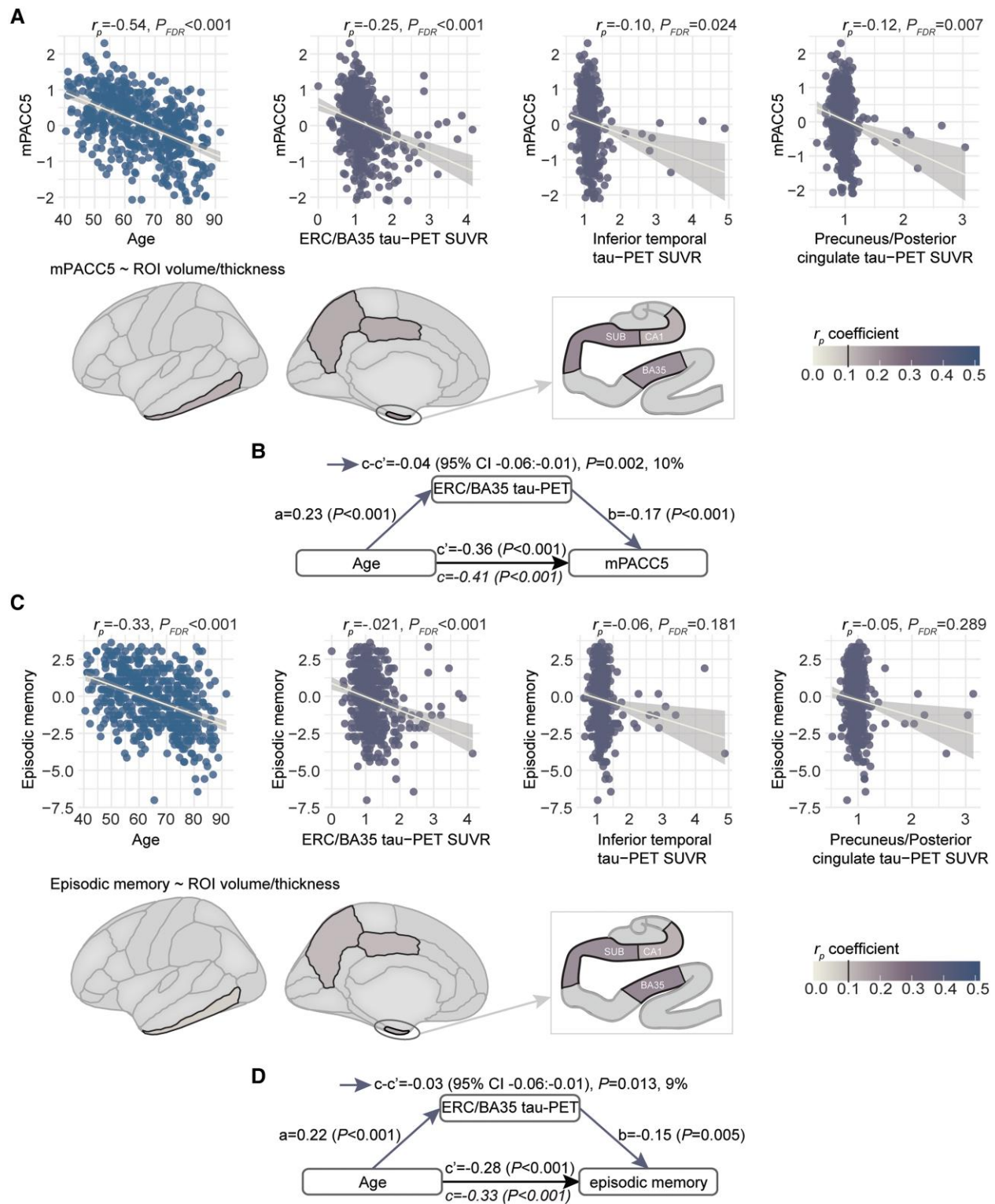
**Figure 3** Age and regional tau-PET  $^{18}\text{F}$ -RO948 uptake associations with regional volume/thickness in the whole sample and A $\beta$ - subgroup. (A) Increasing regional tau-PET SUVR associated with decreased thickness/volume in temporal and parietal regions including sex and regional A $\beta$ -PET signal as covariates. (B) Increasing regional tau-PET SUVR associated with decreased thickness/volume in medial temporal and parietal regions additionally adjusting for age. (C) There is an A $\beta$ -independent effect of regional tau-PET signal on the age-structure associations in the whole group for MTL and parietal regions (paths a and b). The direct effect is reported below the arrow (in italics) going from age to structure. (D) In the A $\beta$ - subgroup, increasing regional tau-PET SUVR is associated with decreased thickness/volume in medial temporal and parietal regions. (E) In the A $\beta$ - subgroup, increasing regional tau-PET SUVR is associated with decreased thickness/volume in medial temporal and parietal regions additionally adjusting for age. (F) In the A $\beta$ - subgroup, there is an A $\beta$ -independent effect of regional tau-PET signal on the age-structure associations for BA35. Models including tau-PET are adjusted for age-independent putamen tau-PET tracer uptake. Pearson partial correlation coefficients  $> 0.10$  are  $P_{\text{FDR}} < 0.05$  (dark outline). Light grey regions were not investigated. Similar results are found using global A $\beta$ -PET. BA = Brodmann area; CA1 = cornu ammonis 1; ERC = entorhinal cortex; MTL = medial temporal lobe; PPC = precuneus/posterior cingulate cortex; ROI = region of interest; SUB = subiculum.

temporal, and precuneus/posterior cingulate cortex thickness were associated with reduced global cognition and episodic memory scores. None of the associations remained statistically significant after adjusting for age. Also, no significant mediation effects were found.

#### Ex vivo: RADC cohort

In the full neuropathological cohort of cognitively unimpaired older adults, age was associated with global cognition ( $\rho_{\text{P}} = -0.17$ ,  $P_{\text{FDR}} < 0.001$ ; [Supplementary Table 9](#) and [Supplementary Fig. 6](#)). Tau





tangles in frontal, parietal, and temporal regions were negatively, but weakly, associated with global cognition ( $r_{ho_p} = -0.10$ – $0.17$ ,  $P_{FDR} = 0.046$ – $0.002$ ). Tau load in temporal regions partially mediated the age-global cognition association (Supplementary Fig. 6; variance explained: 12–29%). Additionally, tau tangles in frontal and temporal regions, but not age, were weakly but significantly associated with episodic memory ( $r_{ho_p} = -0.11$ – $0.21$ ,  $P_{FDR} = 0.030$ – $<0.001$ ).

In the A $\beta$ - subgroup, only higher ERC tau load was associated with reduced episodic memory ( $r_{ho_p} = -0.20$ ,  $P_{FDR} = 0.021$ ; Supplementary Table 9).

### Sensitivity analyses

*In vivo*, the results remained consistent even when excluding individuals with high meningeal/skull tau-PET binding (Supplementary Tables 1–9), using robust regression models (data not shown) or additionally adjusting the analyses for APOE- $\epsilon 4$  carriership (data not shown), and when using CSF A $\beta 42$ /A $\beta 40$  ratio instead of regional A $\beta$ -PET as a covariate (Supplementary Tables 1–9). Results further converged with the primary analyses when using global instead of regional A $\beta$ -PET as a covariate for Pearson partial correlations and mediation models (age-thickness/volume associations: Supplementary Fig. 4; age-cognition associations: mPACC5:  $c-c' = -0.03$ , 95% CI:  $-0.04$ – $-0.01$ ,  $P = 0.010$ , 8%; ADAS:  $c-c' = -0.03$ , 95% CI:  $-0.05$ – $-0.01$ ,  $P = 0.015$ , 9%). Note that age-tau associations in the A $\beta$ - subgroup yielded slightly stronger results (Supplementary Table 3). Finally, tau-PET measures were significantly associated with CSF p-tau181 for all but the motor region in the whole sample and for temporal and frontal regions in the A $\beta$ - subgroup (Supplementary Table 5). While CSF and PET measures are both proxies of tau pathology with their own limitations, the positive correlations between the two supports the use of tau-PET as a proxy of tau pathology in the brain, even in A $\beta$ - cases.

*Ex vivo*, similar results are found when defining the A $\beta$ - subgroup with Thal stages, except for the age and anterior cingulate cortex tangle association ( $r_{ho_p} = 0.09$ ,  $P_{FDR} = 0.454$ ). Moreover, the ERC tau load and episodic memory associations was slightly weaker and not significant ( $r_{ho_p} = -0.16$ ,  $P_{FDR} = 0.248$ ) potentially due to the decreased power in this smaller sample.

## Discussion

We investigated age-related tau-PET deposition patterns and potential downstream effects on brain structure and cognition in a large cohort of cognitively unimpaired older adults as well as in a subgroup with low A $\beta$  levels. Our study highlights two main findings. First, in this cognitively unimpaired sample, the occurrence of age-related tau-PET signal was observed within the MTL but also in several neocortical areas (e.g. inferior temporal, precuneus/posterior cingulate, orbitofrontal, anterior cingulate, inferior parietal, superior frontal) and appeared to be partially independent of A $\beta$ -PET. This was supported by the analyses in the A $\beta$ - subgroup and in the neuropathological cohort, where positive associations between age and tangle density were found in temporal and frontal regions. Second, this partially A $\beta$ -PET-independent age-related tau-PET retention appears to exert downstream effects on structure and cognition within the MTL and, interestingly also in the precuneus/posterior cingulate in our sample. These findings indicate that tau pathology may accumulate outside the MTL in 'normal' ageing and already exerts modest downstream effects on structure and global cognition.

We found a significant age-related increase in tau-PET retention (*in vivo*) and tau tangle density (*ex vivo*) in the MTL in cognitively unimpaired older adults with no or low amounts of A $\beta$ . This is in line with previous *in vivo* PET studies.<sup>21,23</sup> We additionally find similar, albeit weaker, associations outside the MTL. The observation of age-related tau deposition within, and to some extent outside, the MTL in A $\beta$ - individuals is in agreement with the definition of PART,<sup>10</sup> where tau pathology is reported in the insula and inferior temporal gyrus in Braak stages III and IV. However, our findings suggest that age-related tau pathology goes beyond these Braak stage III-IV regions and includes, among others, the anterior and posterior cingulate and the precuneus. The occurrence of tau pathology in more widespread neocortical regions is in line with recent neuropathological studies, which indicate that tau pathology may occur outside the MTL independently of A $\beta$  and widespread tau seeding activity is not confined to the MTL in cognitively unimpaired adults.<sup>15,18-20</sup> In addition, also *in vivo* studies showed tau-PET retention outside the MTL in A $\beta$ - and tau-positive older individuals<sup>62,63</sup> and in cognitively unimpaired individuals with low A $\beta$  levels.<sup>21-23,64,65</sup> Yet, our study uses a second-generation tau-PET tracer and a larger sample size compared to prior *in vivo* studies. While our results suggest that there is tau pathology in these regions independent of A $\beta$  pathology, it is possible that there are individuals in our study which have A $\beta$  pathology not detectable by our methods. It is unlikely that our results were severely impacted by individuals with undetected A $\beta$  pathology since we used a conservative cut-off, adjusted analyses for A $\beta$  levels, and found similar results in the *in vivo* data when using CSF A $\beta$ , which is generally thought to be more sensitive to early A $\beta$  pathology.<sup>66</sup> We additionally found similar results in the neuropathological dataset. However, we likely captured individuals with low A $\beta$  levels, rather than with no A $\beta$ , who can therefore be categorized as possible PART rather than definite PART. We also cannot rule out that some individuals in our A $\beta$ - subgroup will progress to an A $\beta$ -positive status. Therefore, longitudinal investigations are necessary to examine whether these observations would fall on the Alzheimer's disease continuum. Similarly, this study does not allow us to draw conclusions about whether PART is a separate entity or lies on the Alzheimer's disease spectrum.<sup>67,68</sup> Nevertheless, our findings, suggestive of a partially A $\beta$ -independent presence of tau deposition in ageing, additionally highlight the possibility of measuring PART<sup>10</sup> *in vivo* already in preclinical stages. The autoradiography experiment in the current study gives support of the tracer's sensitivity to tau pathology also in PART, albeit likely dependent on the severity and maturity of the tau pathology.

Interestingly, tau-PET signal in the MTL and in medial parietal regions is also associated with volume or cortical thickness measures in the same regions, independent of A $\beta$  pathology, in this group of cognitively unimpaired individuals. The results for the MTL are in line with previous research,<sup>69,70</sup> but extends previous work by showing that the negative effect of ageing on MTL subfields is, independently of A $\beta$ , partially mediated by tau-PET, and by showing that these results hold also in the A $\beta$ - subgroup for BA35. Our results for the medial parietal regions suggest that age-related, A $\beta$ -independent tau pathology is not only present in neocortical regions, but already has negative effects on brain structure. Tau-PET in this parietal region (precuneus/posterior cingulate) appears to partially mediate the age-thickness association. We also found an association of ERC/BA35 tau-PET with cognition in this cognitively unimpaired sample, which adds to the existing literature (e.g.<sup>64,71-73-74</sup>). We extended previous research by showing that tau within the MTL (ERC/BA35) additionally partially mediates

age-related differences in global cognition. No association between the tau-PET signal in the parietal regions and cognition were found, which could reflect lower levels of tau compared to ERC/BA35 tau-PET (Supplementary Table 1) or a relative recent aggregation of tau and, thus, has not exerted an effect on cognition yet. In general the effect sizes are relatively small, indicating that other factors, such as co-pathologies or non-specific age-related changes, potentially mediate the age-structure and age-cognition associations. Though, also methodological limitations of the imaging, pathology, and cognition measures and limitations of mediation models may play a role in the small effect sizes. Notably, in this study, MTL grey matter does not mediate the age-cognition relationship indicating that any structural changes that the MTL is undergoing are either too small to detect using MRI or too small to contribute to cognitive change. Perhaps tau pathology affects cognition in a different way, e.g. through synaptic changes (see Wu et al.<sup>75</sup> for an overview).

The most widely supported hypothesis is that A $\beta$  accumulation is necessary for tau spread/accumulation outside the MTL to take off.<sup>7,8,76</sup> Nevertheless, our findings show that there are tau aggregates independent of A $\beta$  outside the MTL and there are effects of tau pathology on brain structure and function even in cognitively unimpaired individuals. While we cannot make claims about spread based on this cross-sectional data, the findings provide several insights into the notion that A $\beta$  is necessary for tau pathology to spread, albeit not challenging the critical role of A $\beta$  in tau accumulation. First, it may be possible that the subthreshold A $\beta$  levels in our samples are high enough to facilitate the beginning accumulation and/or potential spread of tau outside the MTL.<sup>77</sup> Second, it is conceivable that while there is tau seeding activity<sup>18</sup> and tau pathology in several regions outside the MTL, tau will only accumulate to a limited extent and spread slowly or not at all without the presence of A $\beta$ .<sup>78</sup> Third, it is possible that A $\beta$  and tau pathology accumulate separately<sup>79</sup> until a point where A $\beta$  starts to facilitate tauopathy.<sup>80</sup> While A $\beta$  may trigger tau pathology spread and facilitate accumulation, the findings of this study suggest that tau deposition may occur in the absence of A $\beta$  at lower ranges already in 'healthy' ageing (see also Lowe et al.<sup>22</sup> and Groot et al.<sup>72</sup>), but future longitudinal studies are needed to explore this further.

Our results could also shed light on the so-called spatial disconnection paradox in Alzheimer's disease,<sup>81</sup> the question how A $\beta$  facilitates the spread of tau if the first occurrence of these two pathologies is in different brain regions. Since we found evidence of age-related tau in regions beyond the MTL, both in the *in vivo* and *ex vivo* cohorts, with most pronounced effects in early A $\beta$  regions<sup>40</sup> (precuneus/posterior cingulate) *in vivo*, there may not be a spatial disconnect but tau may start to accumulate outside the MTL independent of A $\beta$ . Whether tau can, independently of A $\beta$ , accumulate in larger quantities or spread across the neocortex, or whether A $\beta$  drives the speed of tau spread, remains to be elucidated by longitudinal studies.

## Strengths and limitations

Strengths of the current study include the use of *in vivo* and neuropathological cohorts, large sample sizes, fine-grained investigation of changes in MTL subfields, and the autoradiography study. The robustness of our findings and the validity of the used *in vivo* measurements are supported, given the consistency of our results when conducting sensitivity analyses and observing A $\beta$ -independent tau *in vivo* and *ex vivo*, despite a large age difference between cohorts. Yet, the results of the study must be interpreted given its limitations. First, the cross-sectional nature of the study does not allow

to conclude causal relationships. Second, the enrichment of APOE- $\epsilon$ 4 allele carriership may limit generalizability. However, other studies with lower percentage of cognitively unimpaired APOE- $\epsilon$ 4 allele carriers reported similar results (e.g. Lowe et al.<sup>22</sup> and Harrison et al.<sup>24</sup>). Third, not all regions investigated *in vivo* were available in the *ex vivo* cohorts (e.g. precuneus/posterior cingulate), potentially limiting the conclusions of the *in vivo* findings. Fourth, mediation models, while useful, have limitations.<sup>82,83</sup> Using different measures (e.g. PET, MRI, cognitive tests), the caveats of these measures are introduced into the mediation models, which may be part of the variance (un-)explained by the models and smaller effect sizes. We reduced this risk by fitting mediation models only for associations previously found significant in the partial correlation analysis. Lastly, since the investigated cognitively unimpaired older adults have low tau-PET SUVRs, it is possible that we capture other age-related changes or co-pathologies, as some uptake may be noise or that the used tau-PET tracer shows some off-target binding.<sup>25</sup> Yet, sensitivity analyses where individuals with high meningeal/skull binding were excluded support our results. Additionally, we adjusted all analyses with tau-PET signal as main predictor/outcome for age-independent putamen uptake, to ensure limited effects of off-target binding (also note Krishnadas et al.<sup>84</sup>), and we used a second-generation tau-PET tracer that shows less off-target binding compared to previous tracers.<sup>25</sup> Lastly, the finding of age-related tau within and outside the MTL in the *ex vivo* cohort, supports that the tau-PET SUVRs findings do not reflect solely age-related noise.

## Conclusion

In this study comprising cognitively unimpaired people, we observe A $\beta$ -independent age-related tau deposition (defined *in vivo* with tau-PET and *ex vivo* neuropathologically) not only in the MTL but also in neocortical regions (*in vivo*: temporal, frontal, and parietal regions; *ex vivo*: MTL, inferior temporal, anterior cingulate cortex). Further *ex vivo* validation in other neocortical regions is still needed, especially for parietal regions. This partially A $\beta$ -PET-independent tau accumulation appears to exert downstream effects on (i) brain structure, again, within and interestingly to a limited extent also outside the MTL; and (ii) cognitive functioning. These insights aid in elucidating the progression of pathophysiology in ageing by indicating an early involvement of low levels of tau in parietal and frontal regions and thereby accumulation that appears to be at least partially A $\beta$  independent. This has implications for understanding the spreading of tau outside the MTL, also in the context of Alzheimer's disease. The results also highlight that tau in the absence of higher levels of A $\beta$  is relevant during aging given its association with atrophy and cognition. This, thereby, highlights the clinical relevance of PART, providing additional impetus to investigate and understand this entity further. Even in the absence of cerebral  $\beta$ -amyloidosis, tau pathology should be considered as a potential cause of at least modest cognitive impairment and atrophy. Thus, the results of our study support the potential benefits of tau-targeting treatments already in preclinical stages in individuals with no or relatively low A $\beta$  levels.

## Acknowledgements

We would like to acknowledge all the BioFINDER team members as well as participants in the study and their family members for their dedication. We want to thank all MAP, ROS, Minority Aging Research Study, and African American Clinical Core participants,



as well as the Rush Alzheimer's Disease Center staff. RADC resources can be requested at <https://www.radc.rush.edu>.

## Funding

This study was supported by MultiPark—A Strategic Research Area at Lund University. Additionally, this work was supported by National Institute of Aging grants R01-AG070592, P30AG010161/P30AG072975, R01AG017917, R01AG22018, R01AG064233, and the Alzheimer's Association (AARF-19-615258). The BioFINDER-2 study was supported by the Swedish Research Council (2016-00906 and 2018-02052), the Knut and Alice Wallenberg foundation (2017-0383), the Marianne and Marcus Wallenberg foundation (2015.0125), the Strategic Research Area MultiPark (Multidisciplinary Research in Parkinson's disease) at Lund University, the Alzheimerfonden (AF-939932), the Swedish Brain Foundation (FO2021-0293 and FO2022-0204), Svenska Parkinsonstiftelsen (1280/20), the Cure Alzheimer's fund, the Konung Gustaf V:s och Drottning Victorias Frimurarestiftelse, Skånes universitetssjukhus (2020-O000028), Region Skåne (2020-0314) and the Swedish federal government under the ALF agreement (2018-Projekt0279). The precursor of <sup>18</sup>F-flutemetamol was sponsored by GE Healthcare. A.P.B. is supported by a postdoctoral fellowship from the Fonds de Recherche du Québec - Santé (298314). The RADC cohorts (ROS/MAP/MARS/AACORE) were supported by National Institutes of Health grants P30AG10161, P30AG72975, R01AG15819, R01AG17917, and R01AG22018. The funding sources had no role in the design and conduct of the study; in the collection, analysis, interpretation of the data; or in the preparation, review or approval of the manuscript.

## Competing interests

S.P. has served on the scientific advisory boards for Hoffman-La Roche and Geras Solutions. O.H. has acquired research support (for the institution) from ADx, AVID Radiopharmaceuticals, Biogen, Eli Lilly, Eisai, Fujirebio, GE Healthcare, Pfizer and Roche. In the past 2 years, he has received consultancy/speaker fees from AC Immune, Amylyx, Alzpath, BioArctic, Biogen, Cerveau, Fujirebio, Genentech, Merck, Novartis, Roche and Siemens. M.H. and S.M. are full-time employees of F. Hoffmann La Roche Ltd. The other authors report no competing interests.

## Supplementary material

[Supplementary material](#) is available at [Brain online](#).

## References

- Hansson O. Biomarkers for neurodegenerative diseases. *Nat Med*. 2021;27:954-963.
- Jack CR Jr, Bennett DA, Blennow K, et al. NIA-AA Research framework: toward a biological definition of Alzheimer's disease. *Alzheimers Dement J Alzheimers Assoc*. 2018;14:535-562.
- Hardy JA, Higgins GA. Alzheimer's disease: the amyloid cascade hypothesis. *Science*. 1992;256:184-185.
- Selkoe DJ, Hardy J. The amyloid hypothesis of Alzheimer's disease at 25 years. *EMBO Mol Med*. 2016;8:595-608.
- Thal DR, Rüb U, Orantes M, Braak H. Phases of A $\beta$ -deposition in the human brain and its relevance for the development of AD. *Neurology*. 2002;58:1791.
- Braak H, Braak E. Neuropathological staging of Alzheimer-related changes. *Acta Neuropathol (Berl)*. 1991;82:239-259.
- Pooler AM, Polydoro M, Maury EA, et al. Amyloid accelerates tau propagation and toxicity in a model of early Alzheimer's disease. *Acta Neuropathol Commun*. 2015;3:14-14.
- Sanchez JS, Becker JA, Jacobs HIL, et al. The cortical origin and initial spread of medial temporal tauopathy in Alzheimer's disease assessed with positron emission tomography. *Sci Transl Med*. 2021;13:eabc0655.
- Vogel JW, Iturria-Medina Y, Strandberg OT, et al. Spread of pathological tau proteins through communicating neurons in human Alzheimer's disease. *Nat Commun*. 2020;11:2612.
- Crary JF, Trojanowski JQ, Schneider JA, et al. Primary age-related tauopathy (PART): a common pathology associated with human aging. *Acta Neuropathol (Berl)*. 2014;128:755-766.
- Jefferson-George KS, Wolk DA, Lee EB, McMillan CT. Cognitive decline associated with pathological burden in primary age-related tauopathy. *Alzheimers Dement J Alzheimers Assoc*. 2017;13:1048-1053.
- Josephs KA, Murray ME, Tosakulwong N, et al. Tau aggregation influences cognition and hippocampal atrophy in the absence of beta-amyloid: A clinico-imaging-pathological study of primary age-related tauopathy (PART). *Acta Neuropathol (Berl)*. 2017;133:705-715.
- Quintas-Neves M, Teylan MA, Besser L, et al. Magnetic resonance imaging brain atrophy assessment in primary age-related tauopathy (PART). *Acta Neuropathol Commun*. 2019;7:204-204.
- Busche MA, Hyman BT. Synergy between amyloid- $\beta$  and tau in Alzheimer's disease. *Nat Neurosci*. 2020;23:1183-1193.
- Kaufman SK, Del Tredici K, Thomas TL, Braak H, Diamond MI. Tau seeding activity begins in the transentorhinal/entorhinal regions and anticipates phospho-tau pathology in Alzheimer's disease and PART. *Acta Neuropathol (Berl)*. 2018;136:57-67.
- Lewis J, Dickson DW. Propagation of tau pathology: Hypotheses, discoveries, and yet unresolved questions from experimental and human brain studies. *Acta Neuropathol (Berl)*. 2016;131:27-48.
- Monsell SE, Mock C, Roe CM, et al. Comparison of symptomatic and asymptomatic persons with Alzheimer disease neuropathology. *Neurology*. 2013;80:2121.
- Furman JL, Vaquer-Alicea J, White CL III, Cairns NJ, Nelson PT, Diamond MI. Widespread tau seeding activity at early Braak stages. *Acta Neuropathol (Berl)*. 2017;133:91-100.
- LaCroix MS, Hitt BD, Beaver JD, et al. Tau seeding without tauopathy. *bioRxiv*. [Preprint] doi:10.1101/2022.02.03.479049
- Meisl G, Hidari E, Allinson K, et al. In vivo rate-determining steps of tau seed accumulation in Alzheimer's disease. *Sci Adv*. 2021;7:eabh1448.
- Schöll M, Lockhart SN, Schonhaut DR, et al. PET Imaging of tau deposition in the aging human brain. *Neuron*. 2016;89:971-982.
- Lowe VJ, Wiste HJ, Senjem ML, et al. Widespread brain tau and its association with ageing, Braak stage and Alzheimer's dementia. *Brain J Neurol*. 2018;141:271-287.
- Jack CR Jr, Wiste HJ, Schwarz CG, et al. Longitudinal tau PET in ageing and Alzheimer's disease. *Brain*. 2018;141:1517-1528.
- Harrison TM, Du R, Klencklen G, Baker SL, Jagust WJ. Distinct effects of beta-amyloid and tau on cortical thickness in cognitively healthy older adults. *Alzheimers Dement*. 2021;17:1085-1096.
- Smith R, Schöll M, Leuzy A, et al. Head-to-head comparison of tau positron emission tomography tracers [<sup>18</sup>F]flortaucipir and [<sup>18</sup>F]RO948. *Eur J Nucl Med Mol Imaging*. 2020;47:342-354.

26. Palmqvist S, Janelidze S, Quiroz YT, et al. Discriminative accuracy of plasma phospho-tau217 for Alzheimer disease vs other neurodegenerative disorders. *JAMA*. 2020;324:772-781.
27. Marquez DX, Glover CM, Lamar M, et al. Representation of older latinxs in cohort studies at the rush Alzheimer's disease center. *Neuroepidemiology*. 2020;54:404-418.
28. Hyman BT, Phelps CH, Beach TG, et al. National institute on aging–Alzheimer's association guidelines for the neuropathologic assessment of Alzheimer's disease. *Alzheimers Dement*. 2012; 8:1-13.
29. Bennett DA, Buchman AS, Boyle PA, Barnes LL, Wilson RS, Schneider JA. Religious orders study and rush memory and aging project. *J Alzheimers Dis*. 2018;64(s1):S161-S189.
30. Mirra SS, Heyman A, McKeel D, et al. The consortium to establish a registry for Alzheimer's disease (CERAD). *Neurology*. 1991;41:479.
31. Berron D, Vieweg P, Hochkeppler A, et al. A protocol for manual segmentation of medial temporal lobe subregions in 7Tesla MRI. *NeuroImage Clin*. 2017;15:466-482.
32. Xie L, Wisse LEM, Pluta J, et al. Automated segmentation of medial temporal lobe subregions on in vivo T1-weighted MRI in early stages of Alzheimer's disease. *Hum Brain Mapp*. 2019;40: 3431-3451.
33. Yushkevich PA, Pluta JB, Wang H, et al. Automated volumetry and regional thickness analysis of hippocampal subfields and medial temporal cortical structures in mild cognitive impairment. *Hum Brain Mapp*. 2015;36:258-287.
34. Xie L, Wisse LEM, Wang J, et al. Deep label fusion: a generalizable hybrid multi-atlas and deep convolutional neural network for medical image segmentation. *Med Image Anal*. 2023;83:102683.
35. Xie L, Wisse LEM, Das SR, et al. Characterizing anatomical variability and Alzheimer's disease related cortical thinning in the medial temporal lobe using graph-based groupwise registration and point set geodesic shooting. *Shap Med Imaging*. 2018;11167: 28–37.
36. Baker SL, Maass A, Jagust WJ. Considerations and code for partial volume correcting [18F]-AV-1451 tau PET data. *Data Brief*. 2017;15:648-657.
37. Thurfjell L, Lilja J, Lundqvist R, et al. Automated quantification of <sup>18</sup>F-flutemetamol PET activity for categorizing scans as negative or positive for brain amyloid: concordance with visual image reads. *J Nucl Med*. 2014;55:1623.
38. Rousset OG, Ma Y, Evans AC. Correction for partial volume effects in PET: principle and validation. *J Nucl Med*. 1998;39: 904-911.
39. Leuzy A, Smith R, Ossenkoppele R, et al. Diagnostic performance of RO948 F 18 tau positron emission tomography in the differentiation of Alzheimer disease from other neurodegenerative disorders. *JAMA Neurol*. 2020;77:955-965.
40. Palmqvist S, Schöll M, Strandberg O, et al. Earliest accumulation of  $\beta$ -amyloid occurs within the default-mode network and concurrently affects brain connectivity. *Nat Commun*. 2017;8:1214.
41. Ziontz J, Bilgel M, Shafer AT, et al. Tau pathology in cognitively normal older adults. *Alzheimers Dement Amst Neth*. 2019;11: 637-645.
42. Hansson O, Batrla R, Brix B, et al. The Alzheimer's association international guidelines for handling of cerebrospinal fluid for routine clinical measurements of amyloid  $\beta$  and tau. *Alzheimers Dement*. 2021;17:1575-1582.
43. Janelidze S, Stomrud E, Brix B, Hansson O. Towards a unified protocol for handling of CSF before  $\beta$ -amyloid measurements. *Alzheimers Res Ther*. 2019;11:63.
44. Hansson O, Seibyl J, Stomrud E, et al. CSF Biomarkers of Alzheimer's disease concord with amyloid- $\beta$  PET and predict clinical progression: a study of fully automated immunoassays in BioFINDER and ADNI cohorts. *Alzheimers Dement*. 2018;14: 1470-1481.
45. Lifke V, Kollmorgen G, Manuilova E, et al. Elecsys® total-tau and phospho-tau (181P) CSF assays: analytical performance of the novel, fully automated immunoassays for quantification of tau proteins in human cerebrospinal fluid. *Alzheimer's Dis Mak Point*. 2019;72:30-38.
46. Papp KV, Rentz DM, Orlovsky I, Sperling RA, Mormino EC. Optimizing the preclinical Alzheimer's cognitive composite with semantic processing: The PACC5. *Alzheimers Dement Transl Res Clin Interv*. 2017;3:668-677.
47. Folstein MF, Folstein SE, McHugh PR. "Mini-mental state": a practical method for grading the cognitive state of patients for the clinician. *J Psychiatr Res*. 1975;12:189-198.
48. Connor DJ, Sabbagh MN. Administration and scoring variance on the ADAS-cog. *J Alzheimers Dis*. 2008;15:461-464.
49. Smith A. *Symbol digit modalities test*. Western psychological services; 1973.
50. Pichet Binette A, Franzmeier N, Spotorno N, et al. Amyloid-associated increases in soluble tau relate to tau aggregation rates and cognitive decline in early Alzheimer's disease. *Nat Commun*. 2022;13:6635.
51. Bennett DA, Schneider JA, Buchman AS, Mendes de Leon C, Bienias JL, Wilson RS. The rush memory and aging project: Study design and baseline characteristics of the study cohort. *Neuroepidemiology*. 2005;25:163-175.
52. De Jager PL, Shulman JM, Chibnik LB, et al. A genome-wide scan for common variants affecting the rate of age-related cognitive decline. *Neurobiol Aging*. 2012;33:1017.e1-1017.e15.
53. Wilson RS, Arnold SE, Schneider JA, Tang Y, Bennett DA. The relationship between cerebral Alzheimer's disease pathology and odour identification in old age. *J Neurol Neurosurg Amp Psychiatry*. 2007;78:30.
54. Schneider JA, Aggarwal NT, Barnes L, Boyle P, Bennett DA. The neuropathology of older persons with and without dementia from community versus clinic cohorts. *J Alzheimers Dis*. 2009; 18:691-701.
55. R Core Team. R: a language and environment for statistical computing. Published online 2020. <https://www.R-project.org/>
56. Kim S. ppcor: Partial and Semi-Partial (Part) Correlation. Published online 2015. <https://CRAN.R-project.org/package=ppcor>
57. Rosseeuw Y. Lavaan: an R package for structural equation modeling. *J Stat Softw*. 2012;48:1-36.
58. Pichet Binette A, Franzmeier N, Spotorno N, et al. Amyloid-associated increases in soluble tau is a key driver in accumulation of tau aggregates and cognitive decline in early Alzheimer. *medRxiv*. [Preprint] doi: 10.1101/2022.01.07.22268767
59. Venables WN, Ripley BD. *Modern applied statistics with S*. 4th ed. Springer; 2002.
60. Koenker R. quantreg: Quantile Regression. R package version 5.75. Published online 2020. <https://CRAN.R-project.org/package=quantreg>
61. Rousseeuw PJ, Leroy AM. *Robust regression and outlier detection*. Wiley; 1987.
62. Weigand AJ, Bangen KJ, Thomas KR, et al. Is tau in the absence of amyloid on the Alzheimer's continuum? A study of discordant PET positivity. *Brain Commun*. 2020;2:fcz046.
63. Yoon B, Guo T, Provost K, et al. Abnormal tau in amyloid PET negative individuals. *Neurobiol Aging*. 2022;109:125-134.
64. Chen X, Cassady KE, Adams JN, Harrison TM, Baker SL, Jagust WJ. Regional tau effects on prospective cognitive change in cognitively normal older adults. *J Neurosci*. 2021;41:366.

65. Maass A, Berron D, Harrison TM, et al. Alzheimer's pathology targets distinct memory networks in the ageing brain. *Brain*. 2019;142:2492-2509.
66. Palmqvist S, Mattsson N, Hansson O, for the Alzheimer's Disease Neuroimaging Initiative. Cerebrospinal fluid analysis detects cerebral amyloid- $\beta$  accumulation earlier than positron emission tomography. *Brain*. 2016;139:1226-1236.
67. Duyckaerts C, Braak H, Brion JP, et al. PART Is part of Alzheimer disease. *Acta Neuropathol (Berl)*. 2015;129:749-756.
68. Hickman RA, Flowers XE, Wisniewski T. Primary age-related tauopathy (PART): Addressing the Spectrum of neuronal tauopathic changes in the aging brain. *Curr Neurol Neurosci Rep*. 2020;20:39.
69. Berron D, Vogel JW, Insel PS, et al. Early stages of tau pathology and its associations with functional connectivity, atrophy and memory. *Brain*. 2021;144:2771-2783.
70. de Flores R, Wisse LEM, Das SR, et al. Contribution of mixed pathology to medial temporal lobe atrophy in Alzheimer's disease. *Alzheimers Dement*. 2020;16:843-852.
71. Lowe VJ, Bruinsma TJ, Wiste HJ, et al. Cross-sectional associations of tau-PET signal with cognition in cognitively unimpaired adults. *Neurology*. 2019;93:e29-e39.
72. Groot C, Doré V, Robertson J, et al. Mesial temporal tau is related to worse cognitive performance and greater neocortical tau load in amyloid- $\beta$ -negative cognitively normal individuals. *Neurobiol Aging*. 2021;97:41-48.
73. Maass A, Lockhart SN, Harrison TM, et al. Entorhinal tau pathology, episodic memory decline, and neurodegeneration in aging. *J Neurosci Off J Soc Neurosci*. 2018;38:530-543.
74. Tideman P, Stomrud E, Leuzy A, Mattsson-Carlgrén N, Palmqvist S, Hansson O. Association of  $\beta$ -amyloid accumulation with executive function in adults with unimpaired cognition. *Neurology*. 2022;98:e1525.
75. Wu M, Zhang M, Yin X, et al. The role of pathological tau in synaptic dysfunction in Alzheimer's diseases. *Transl Neurodegener*. 2021;10:45.
76. Adams JN, Maass A, Harrison TM, Baker SL, Jagust WJ. Cortical tau deposition follows patterns of entorhinal functional connectivity in aging. *eLife*. 2019;8:e49132.
77. Guo T, Landau SM, Jagust WJ, for the Alzheimer's Disease Neuroimaging Initiative. Age, vascular disease, and Alzheimer's disease pathologies in amyloid negative elderly adults. *Alzheimers Res Ther*. 2021;13:174.
78. Kametani F, Hasegawa M. Reconsideration of amyloid hypothesis and tau hypothesis in Alzheimer's disease. *Front Neurosci*. 2018;12:25.
79. Spires-Jones TL, Attems J, Thal DR. Interactions of pathological proteins in neurodegenerative diseases. *Acta Neuropathol (Berl)*. 2017;134:187-205.
80. Frisoni GB, Altomare D, Thal DR, et al. The probabilistic model of Alzheimer disease: The amyloid hypothesis revised. *Nat Rev Neurosci*. 2022;23:53-66.
81. van der Kant R, Goldstein LSB, Ossenkoppele R. Amyloid- $\beta$ -independent regulators of tau pathology in Alzheimer disease. *Nat Rev Neurosci*. 2020;21:21-35.
82. Gunzler D, Chen T, Wu P, Zhang H. Introduction to mediation analysis with structural equation modeling. *Shanghai Arch Psychiatry*. 2013;25:390-394.
83. Rijnhart JJM, Lamp SJ, Valente MJ, MacKinnon DP, Twisk JWR, Heymans MW. Mediation analysis methods used in observational research: A scoping review and recommendations. *BMC Med Res Methodol*. 2021;21:226.
84. Krishnadas N, Doré V, Groot C, et al. Mesial temporal tau in amyloid- $\beta$ -negative cognitively normal older persons. *Alzheimers Res Ther*. 2022;14:51-51.